

RESEARCH ARTICLE

Frontostriatal network dysfunction as a domain-general mechanism underlying phantom perception

Jeffrey Hullfish¹  | Ian Abenes¹ | Hye Bin Yoo¹ | Dirk De Ridder² | Sven Vanneste^{1,3}

¹School of Behavioral and Brain Sciences, The University of Texas at Dallas, Richardson, Texas

²Department of Surgical Sciences, Dunedin School of Medicine, University of Otago, Dunedin, New Zealand

³Global Brain Health Institute, Institute of Neuroscience, Trinity College Dublin, Dublin, Ireland

Correspondence

Sven Vanneste, Lab for Clinical & Integrative Neuroscience, School of Behavioral & Brain Sciences, University of Texas at Dallas, 800 W Campbell Rd, Richardson, TX 75080.
Email: sven.vanneste@utdallas.edu

Funding information

NIH Blueprint for Neuroscience Research, Grant/Award Number: 1U54MH091657; McDonnell Center for Systems Neuroscience

Abstract

In the present study, we use resting state fMRI to investigate whether nucleus accumbens (NAc) and extended frontostriatal networks are involved in the pathology of auditory phantom perception, i.e., tinnitus, through a study of functional connectivity. We hypothesize that resting state functional connectivity involving NAc will be increased relative to what is observed in healthy subjects and that this connectivity will correlate with clinical measures of tinnitus such as percept loudness, duration of symptoms, etc. We show that a large sample of patients with chronic tinnitus ($n = 90$) features extensive functional connectivity involving NAc that is largely absent in healthy subjects ($n = 94$). We further show that connectivity involving NAc correlates significantly with tinnitus percept loudness and the duration of tinnitus symptoms, even after controlling for the effects of age and hearing loss. The loudness correlation, which involves NAc and parahippocampal cortex, is consistent with existing literature identifying the parahippocampus as a tinnitus generator. Our results further suggest that frontostriatal connectivity may predict the transition from acute to chronic tinnitus, analogous to what is seen in the pain literature. We discuss these ideas and suggest fruitful avenues for future research.

KEYWORDS

connectivity, fMRI, nucleus accumbens, pain, phantom perception, tinnitus

1 | INTRODUCTION

Phantom perception is defined as sensory experience occurring in the absence of a corresponding external stimulus. Simple phantoms such as tinnitus (i.e., simple auditory phantom perception) are among the most common, chronically affecting one in five adults (Elgoyhen et al., 2015). Phantom perception as a broader category, however, describes phenomena that vary starkly in complexity (Vanneste, Song, & De Ridder, 2013) and can occur in any sensory domain (Mohan & Vanneste, 2017). Despite this, there is a mounting body of evidence that phantoms nevertheless have much in common. Researchers have drawn parallels between tinnitus and chronic pain, for example, since at least the late 80s (Tonndorf, 1987) and these ideas remain a fixture of contemporary research on the subject; see e.g., (Rauschecker, May, Maudoux, & Ploner, 2015; De Ridder, Elgoyhen, Romo, & Langguth, 2011). Fundamental to this argument is the observation that they elicit activity within a vast network of brain regions, as opposed to only the relevant sensory cortex

(De Ridder et al., 2014b; Sedley, Friston, Gander, Kumar, & Griffiths, 2016). While such networks are incompletely understood, the general idea that phantom perceptual experiences are network phenomena is a matter of consensus. The present study aims to improve our understanding of such networks by looking specifically at frontostriatal circuits—networks featuring connectivity between prefrontal cortex and the ventral striatum, specifically nucleus accumbens (NAc)—in the context of tinnitus.

NAc is a subcortical structure that, together with the olfactory tubercle, comprises the ventral part of the striatum, a major component of the basal ganglia (Cauda et al., 2011). Functionally, perhaps its best-known role is as a component of the mesolimbic pathway, a mid-brain dopaminergic system responsible for reward signaling in conjunction with the ventral tegmental area (VTA); see e.g., (Lammel et al., 2012; Navratilova et al., 2012; Schiffer, Waszak, & Yeung, 2015). The literature further implicates NAc in a diverse array of other functions. These include motivation, salience, aversion, sensory gating, and reinforcement learning, among others (Becerra & Borsook, 2008;

Blum et al., 2000; Donoso, Collins, & Koechlin, 2014; Kahn & Shohamy, 2013; Keiflin & Janak, 2015; Koechlin, 2016; Liu, Hairston, Schrier, & Fan, 2011; Rauschecker et al., 2015; De Ridder et al., 2016; Rolland et al., 2015; Takahashi, Schoenbaum, & Niv, 2008; Takahashi et al., 2017).

The only previous research directly assigning a role for NAc in the pathology of tinnitus posits that NAc and ventromedial prefrontal cortex/subgenual anterior cingulate cortex (vmPFC/sgACC) form a frontostriatal gating circuit (Leaver et al., 2011; Leaver et al., 2016; Rauschecker et al., 2015). This putative gatekeeping system is responsible for assigning subjective value or affective meaning to sensory signals and ultimately to trigger action to minimize negative signals (Rauschecker et al., 2015). Per the frontostriatal gating theory, which the authors apply both to tinnitus and to chronic pain, dysfunction in this circuit may affect perception in two nonmutually exclusive ways. Damage to the descending projection from vmPFC/sgACC to the thalamic reticular nucleus could prevent the suppression of irrelevant sensory signals, such as those that result in a phantom percept; this could increase the intensity of such percepts (Rauschecker et al., 2015). Damage to the frontostriatal circuit itself or changes to its inputs could adversely affect the evaluation of stimuli, for example, by assigning negative meaning to neutral stimuli.

Dysfunction in frontostriatal circuits has also been reported elsewhere in the pain literature. For example, functional connectivity between NAc and medial prefrontal cortex (mPFC) appears to be causally involved in the transition from acute to chronic pain, based on evidence from a longitudinal and cross-sectional study (Baliki et al., 2012). The authors of that study suggest that the link between frontostriatal connectivity and pain persistence are evidence of learning processes that play a role in mediating pain chronification (Baliki et al., 2012). The same group also reports that this circuit, which extends into other regions such as anterior cingulate cortex and the insula that are included in the frontostriatal gating theory (Rauschecker et al., 2015), directly correlates with the magnitude of pain intensity and also relates to pain suffering (Apkarian, Hashmi, & Baliki, 2011; see e.g., Figures 9B and 14).

The specific aim of the present study is to investigate empirically whether frontostriatal circuits (especially NAc) are involved in tinnitus and, if so, what their role might be. To this end, we conduct an analysis of resting state functional connectivity (rsFC) on MRI data previously collected from a large sample of the chronic tinnitus population as well as a similarly sized sample of healthy subjects. Functional connectivity in frontostriatal circuits reportedly correlates with phantom pain perception, as discussed previously (Apkarian et al., 2011; Baliki et al., 2006; Baliki et al., 2012), and we hypothesize that an analogous relationship with tinnitus will emerge in our present study. We specifically hypothesize that NAc will exhibit increased rsFC involving ventromedial and orbital regions of prefrontal cortex, which feature some of the main afferent projections to NAc (Cauda et al., 2011). We may however also see rsFC between NAc and anterior regions of cingulate cortex as well as subcortical nuclei such as the amygdala and VTA that are all reportedly part of an extended frontostriatal network (Apkarian et al., 2011; Baliki et al., 2012; Rauschecker et al., 2015). Beyond these group-level comparisons, we will also conduct analyses within the tinnitus group exclusively to test these relationships further.

Specifically, we will correlate NAc-related rsFC (i.e., between NAc and several regions of interest) with subjective, patient-reported measures of the tinnitus subjects, including tinnitus loudness, tinnitus-related distress, hearing loss, and duration of tinnitus symptoms.

2 | MATERIALS AND METHODS

The present study is a retrospective analysis of resting state functional connectivity (rsFC) based on archival fMRI data collected in a clinical context from outpatients with chronic tinnitus. Per the Declaration of Helsinki (World Medical Association, 2000), all subjects were informed about the purpose and procedure of the study and gave their written consent. The local ethical committee of the University of Antwerp Hospital approved the study. We additionally included a set of healthy subjects from the Human Connectome Project (HCP) for post hoc comparison (Van Essen et al., 2012). All coauthors have read and signed the HCP Open Access Data Use agreement, the terms of which are online (<https://store.humanconnectome.org/data/data-use-terms/open-access.php>).

2.1 | Subjects

The primary subject group consisted of chronic tinnitus outpatients ($n = 90$; $n_{\text{male}} = 59$, $n_{\text{female}} = 31$; mean age = 47.8 ± 13.8 [SD] years). The multidisciplinary Tinnitus Research Initiative (TRI) Clinic of the University Hospital of Antwerp, Belgium oversaw the patients. Exclusion criteria were pulsatile tinnitus ("objective tinnitus"), Ménière's disease, otosclerosis, chronic headache, neurological disorders, as well as individuals undergoing treatment for mental disorders.

The comparison group consisted of healthy subjects ($n = 94$; $n_{\text{male}} = 49$, $n_{\text{female}} = 45$; mean age = 28.7 ± 3.8 [SD] years) from the Washington University–University of Minnesota Consortium of the Human Connectome Project (WU-Minn HCP). We chose the subjects with MEG data because that group was roughly equal in size to our primary group, although we did not use the MEG data itself in the present study.

2.2 | Audiological and behavioral assessments of tinnitus subjects

Professionally trained audiologists examined each tinnitus patient to determine the extent of their hearing loss. They measured hearing thresholds (in decibels hearing level, dB HL) at 0.125, 0.25, 0.5, 1, 2, 3, 4, 6, and 8 kHz using pure tone audiometry per the British Society of Audiology guidelines (British Society of Audiology, 2017). For the purposes of this study, the mean hearing loss for each patient is the numerical average of hearing thresholds across both ears and all frequencies.

In addition to their age and the duration of their tinnitus symptoms, patients also reported subjective characteristics of their tinnitus, including percept loudness and tinnitus-related distress. Patients self-reported tinnitus percept loudness using a 0–10 numeric rating scale (NRS), with higher numbers indicating a louder percept (0 = "no tinnitus"). Patients also self-reported tinnitus-related distress using the

Tinnitus Questionnaire (TQ; Hallam, Jakes, & Hinchcliffe, 1988). The TQ ranges in score from 0 to 82, with higher scores corresponding to greater levels of distress. Patients used a validated Dutch translation (Meeus, Blavie, & Van De Heyning, 2007). Summary statistics for these data (age, mean hearing loss, duration, loudness, and distress) are presented as boxplots in Figure 1 along with a comparison of the age data between the tinnitus and healthy subjects.

2.3 | Magnetic resonance imaging

2.3.1 | Acquisition

For the tinnitus subjects, T1-weighted structural images were acquired using a high-resolution scan (MPRAGE) protocol via the 3.0 Tesla Siemens Trio scanner. The scanning protocol used a repetition time (TR) of 2,300 ms, an echo time (TE) of 2.94 ms, an inversion time (TI) of 900 ms, and a flip angle of 9° . One hundred and sixty sagittal slices were taken using a matrix size of $256 \times 256 \text{ mm}^2$ at a resolution of $1 \times 1 \times 1 \text{ mm}^3$. Resting-state functional MRI (rs-fMRI) images were obtained using an echo-planar imaging (EPI) protocol with online motion correction. TR was set at 3000 ms, TE at 30 ms, and the flip angle at 90° . Fifty axial slices were taken and 140 time points were sampled at a resolution of $2.5 \times 2.5 \times 2.8 \text{ mm}^3$. The slice duration was 59.85 ms and the acquisition order was descending. Three volumes were removed from the beginning of each scan to remove saturation effects.

For the HCP subjects, T1-weighted structural images were acquired using a 3D MPRAGE protocol via the 3.0 Tesla Siemens Skyra scanner. This protocol used a TR of 2,400 ms, a TE of 2.14 ms, a TI of 1,000 ms, and a flip angle of 8° . The matrix size was $224 \times 224 \text{ mm}^2$ at a resolution of $0.7 \times 0.7 \times 0.7 \text{ mm}^3$. Rs-fMRI images were obtained using a gradient-echo EPI protocol with TR set at 720 ms, TE at 33.1 ms, the flip angle at 52° . Seventy-two axial slices were taken and 1,200 time points were sampled at a resolution of $2.0 \times 2.0 \times 2.0 \text{ mm}^3$. Five volumes were removed from the beginning of each scan to remove saturation effects (<https://wiki.humanconnectome.org/display/PublicData/Understanding+Timing+Information+in+HCP+Physiological+Monitoring+Files>). Additionally, the multiband factor was set at eight (Smith et al., 2013; Uğurbil et al., 2013). While this scanning protocol differs from that of the

tinnitus group, an inevitable reality of retrospective analysis, there is a precedent in the literature for comparing across data sets in this way; see for example, (Zhang & Li, 2014). We also took steps to maximize consistency across these data sets during preprocessing (see Section 2.3.2).

2.3.2 | Preprocessing

For the tinnitus subjects, MR images were preprocessed using Statistical Parametric Mapping (SPM12b, Wellcome Department of Imaging Neuroscience, University College London, UK). High-resolution structural images (T1) were normalized to the standard MNI template and segmented for three structural components: gray matter, white matter, and cerebrospinal fluid. The functional images (rs-fMRI) were realigned to correct for motion artifacts and coregistered to the corresponding T1 images. Volumes that contained extreme movements were linearly regressed out as covariates using the Artifact Detection Tool (Gabrieli Lab, MIT, US, http://www.nitrc.org/projects/artifact_detect/) as implemented in the CONN toolbox with a 97th-percentile threshold. Functional images were normalized to the standard MNI template using nonlinear transformation parameters acquired by normalizing structural images to standard templates (Ashburner & Friston, 1999; Friston et al., 1995). The images were further processed to account for motion-related and physiological noise using independent component analysis in CONN functional connectivity toolbox (Whitfield-Gabrieli & Nieto-Castanon, 2012). White matter and cerebrospinal fluid signals were considered as confounds and linearly regressed out of the global signal using aCompCor (Behzadi, Restom, Liau, & Liu, 2007). The time series was bandpass filtered in the range of 0.01–0.17 Hz; the upper limit was chosen based on the fact that the Nyquist frequency is the sampling rate ($1/\text{TR} = 0.33 \text{ Hz}$) divided by two ($0.33/2 = 0.167 \text{ Hz}$, rounded up to 0.17 Hz).

For the HCP subjects, we used MR images that were minimally preprocessed via the pipeline described in Glasser et al. (2013), which includes distortion rectification, movement realignment, field map correction, normalization to standard MNI template, minimal high-pass filtering by 0.0005 Hz, denoising based on independent component analysis (Salimi-Khorshidi et al., 2014), and brain extraction. We also added preprocessing steps to maximize the consistency of the HCP

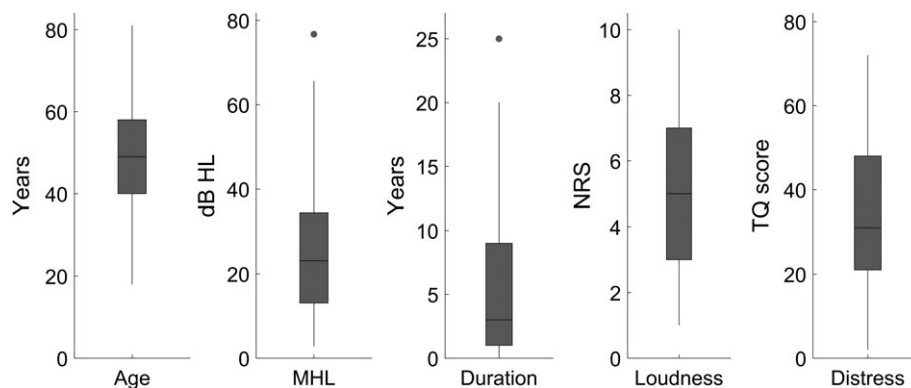


FIGURE 1 Boxplots displaying the summary statistics for the tinnitus patient characteristics and behavioral data. From left to right, the boxplots display age, mean hearing loss (dB HL), the duration of tinnitus symptoms, tinnitus percept loudness (0–10 numeric rating scale), and tinnitus-related distress (TQ score). The line in the center of each box indicates the mean, the outer lines of each box indicate the interquartile range, and the whiskers indicate the full range of the data excluding any outliers, which are indicated by dots

data set with that of our tinnitus patients. Preprocessed functional images were corrected for excessive motion using the Artifact Detection Tool (see Supporting Information). We also segmented the normalized structural images into gray matter, white matter, and cerebrospinal fluid. The white matter and cerebrospinal fluid signals were then treated as confounds and regressed out using aCompCor. Finally, the HCP data were bandpass filtered in the same range of 0.01–0.17 Hz.

2.4 | Regions of interest

We defined several regions of interest (ROIs) for the purposes of rsFC analysis. The time series of the rs-fMRI signal in each ROI is defined as the average time series across all voxels contained within that ROI.

We used the Automated Anatomical Labelling 2 atlas (AAL2) to parcellate the whole brain, including various subcortical nuclei and the cerebellum, into 120 ROIs (Rolls, Joliot, & Tzourio-Mazoyer, 2015); see also (Tzourio-Mazoyer et al., 2002) for the original AAL atlas. The ROIs of the AAL2 atlas were used to calculate whole-brain ROI–ROI rsFC (Section 2.5.1) as well as our NAc–ROI rsFC analyses (Section 2.5.2). We chose this particular atlas because it defines several specific subregions of orbitofrontal cortex (OFC), which is a major source of afferent projections to NAc (Cauda et al., 2011).

Since the AAL2 atlas does not include specific ROIs for NAc, we additionally defined two 3-mm-radius spherical ROIs (i.e., for left and right NAc) using center coordinates obtained from the literature (Cauda et al., 2011) and converted from Talairach to MNI space using an online calculator (<http://sprout022.sprout.yale.edu/mni2tal/mni2tal.html>). We used these ROIs as seed regions for further analyses; see Sections 2.5.2 and 2.5.3.

Finally, we defined 3-mm-radius spherical ROIs ($n = 12$; 6 left, 6 right) for several prominent brain areas identified in the tinnitus literature (Rauschecker et al., 2015; De Ridder et al., 2011; De Ridder, Vanneste, & Freeman, 2014a; De Ridder, Vanneste, Weisz, et al., 2014b): the amygdala, pregenual anterior cingulate cortex (pgACC), subgenual ACC (sgACC), ventromedial prefrontal cortex (vmPFC), primary auditory cortex (A1), and parahippocampal cortex (PHC). We used Neurosynth (<http://neurosynth.org>) to search for these specific regions using term-based meta-analyses. We chose center coordinates for each ROI manually based on the voxel that had the highest Z score and then inverted the x-coordinate to obtain the contralateral ROI. See Table 1 for the center coordinates of all spherical ROIs, including NAc. We used these ROIs together with our NAc ROIs to perform correlation analyses between NAc-related connections and the tinnitus group's behavioral data; see Section 2.5.4.

2.5 | Analysis

We conducted all analyses in: (a) CONN, a third-party Matlab toolbox (Whitfield-Gabrieli & Nieto-Castanon, 2012); (b) in Matlab directly (The MathWorks Inc., 2016); (c) in SPSS (IBM Corp., 2013); and/or (d) in Python. All functions explicitly mentioned in the text are Matlab functions, and the full documentation for each function can be found by searching its name on the MathWorks website (<https://www.mathworks.com/help/>).

TABLE 1 Regions of interest, center coordinates in MNI space

Region	Hemisphere	x	y	z
Nucleus accumbens	Left	−10	12	−13
	Right	13	11	−13
Amygdala	Left/right	±24	−6	−18
Anterior cingulate cortex				
Pregenual ACC	Left/right	±4	38	4
Subgenual ACC	Left/right	±4	26	−10
Auditory cortex	Left/right	±52	−20	6
Parahippocampal cortex	Left/right	±26	−36	−10
Ventromedial PFC	Left/right	±3	44	−8

2.5.1 | Whole-brain ROI–ROI rsFC

Because the tinnitus and control groups utilized different scanning protocols, it was necessary to account for possible scanner-related confounds when performing between-subjects analyses of rsFC. To this end, our first analysis step was to calculate whole-brain rsFC so that we could control for group-level differences in overall connectivity when analyzing group-level differences in NAc-related connectivity.

We analyzed whole-brain rsFC at the subject level in the CONN toolbox using the ROIs of the AAL2 atlas. We then extracted the subject-level rsFC data from CONN as numeric matrices; CONN reports connectivity using Z, i.e., Pearson's *R* with Fisher's Z transformation. Using these matrices, we calculated whole-brain rsFC as the average rsFC across all unique ROI–ROI connections on a per-subject basis. This produced two column vectors of whole-brain rsFC, i.e., one for tinnitus and one for controls, which we used as covariates in our between-subjects analyses of NAc-related rsFC; see Sections 2.5.2 and 2.5.3.

2.5.2 | NAc seed–ROI rsFC

We analyzed rsFC between the left/right NAc seed regions and the ROIs of the AAL2 atlas for both the tinnitus subjects and the healthy subjects (both controlled for the effects of age and whole-brain rsFC) using the CONN toolbox. We extracted the rsFC data for both seeds and both groups and visualized it all using a single ring connectogram (Figure 2), which we created using NeuroMARvL (<http://immersive.erc.monash.edu.au/neuromarvl/>). We then performed a subtraction analysis between the two groups (tinnitus > controls; Figure 3) and tested the difference in rsFC (i.e., ΔZ) for significance at the FDR-corrected 0.05 level.

2.5.3 | NAc seed–voxel rsFC

We analyzed rsFC between the left/right NAc seed regions and the whole brain at the voxel level, controlling for the effects of age and whole-brain rsFC, using the CONN toolbox. After checking the voxel-wise rsFC for significance at the 0.05 level (cluster size threshold; FDR-corrected), we presented the results using glass-brains from the Python module, `nilearn` (https://nilearn.github.io/modules/generated/nilearn.plotting.plot_glass_brain.html). We additionally performed a subtraction analysis between the two groups (tinnitus > controls), thresholding the SPM of the subtraction such that only voxels with significant rsFC differences at the uncorrected 0.0001 level were included in the final

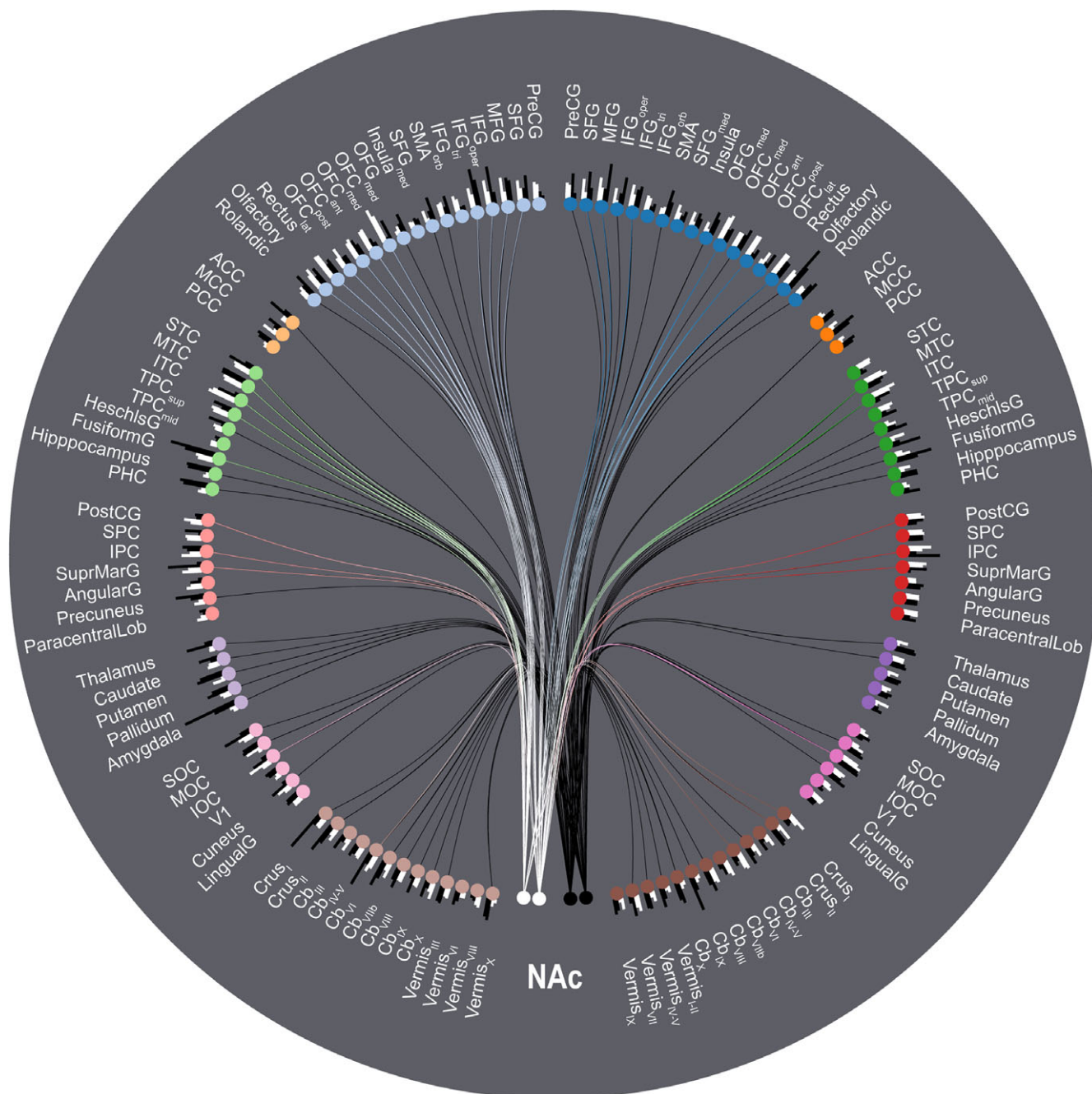


FIGURE 2 Ring connectogram summarizing the rsFC between NAc and the rest of the brain parcellated using the AAL2 atlas. The analysis includes covariates for both age and whole-brain overall rsFC. The two white nodes at six o'clock represent the left and right NAc seed regions in the tinnitus group; the two adjacent black nodes represent the same regions in the control group. The remaining nodes represent AAL2 atlas ROIs separated by hemisphere and then grouped according to the following subdivisions: frontal cortex, cingulate cortex, temporal cortex, parietal cortex, subcortical nuclei, occipital cortex, and the cerebellum. Blue nodes represent frontal ROIs in the right hemisphere; pale blue nodes represent frontal ROIs in the left hemisphere, etc. Note however that the cerebellar vermis ROIs are located at the midline and have been divided between the two cerebellar groups for the sake of symmetry. Bars at each node represent the relative connectivity strength between the NAc seeds/subject groups and each AAL2 ROI. For the sake of legibility, only the upper 30th percentile of edges with connection strengths significant at the FDR-corrected 0.05 level are displayed [Color figure can be viewed at wileyonlinelibrary.com]

result. This subtraction was also plotted as a glass brain and presented alongside the within-group results in Figure 4.

2.5.4 | NAc rsFC correlation analysis

We analyzed rsFC between the left/right NAc seed regions and key tinnitus network ROIs (left/right amygdala, A1, pgACC, sgACC, PHC,

and vmPFC), specifically to look for correlations between each of these connections and the tinnitus patient characteristics (age, mean hearing loss, duration of symptoms, tinnitus loudness, and tinnitus-related distress). We further analyzed partial correlations between these connections and duration/loudness/distress, controlling for the effects of both age and mean hearing loss. We checked all correlations

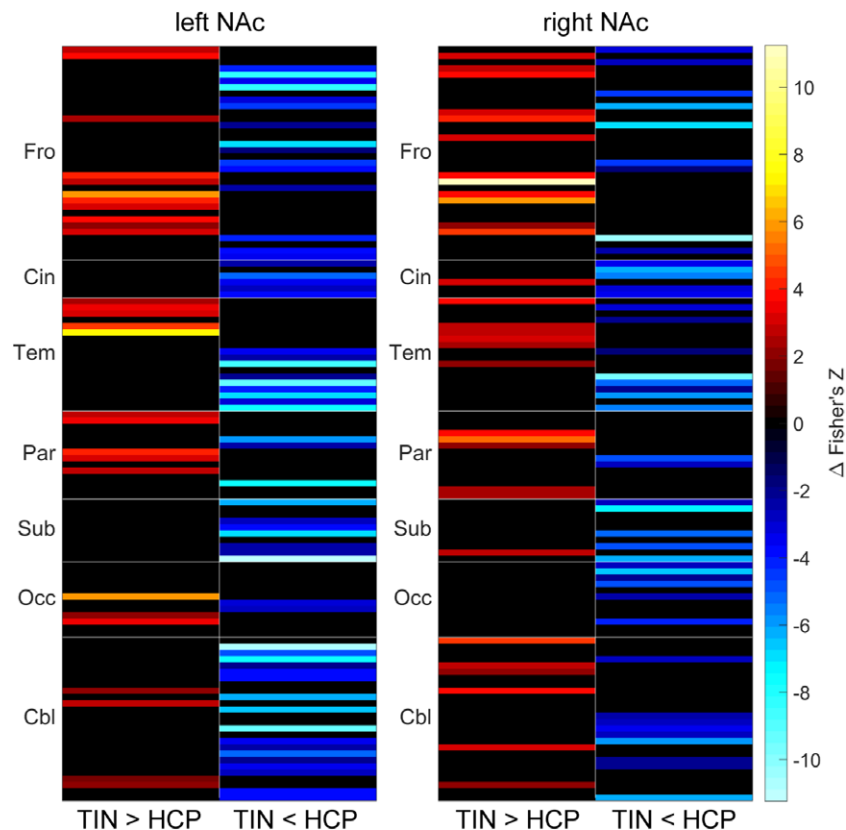


FIGURE 3 Subtraction analysis (TIN > HCP, i.e., tinnitus > controls) of rsFC between left/right NAc and the rest of the brain parcellated using the AAL2 atlas. The analysis includes covariates for both age and whole-brain overall rsFC. Results are presented as heatmaps that have been separated into columns displaying where rsFC is increased (left; warm colors) or decreased (right; cool colors) in tinnitus subjects relative to controls. Displayed results are significant at the 0.05 level, including the FDR correction for multiple comparisons; results that did not reach significance were manually set to zero (=black) [Color figure can be viewed at wileyonlinelibrary.com]

and partial correlations for significance at the 0.05 level, both uncorrected and FDR-corrected using the Benjamini–Hochberg method via `mafdr()` (Hochberg & Benjamini, 1995). The significant (partial) correlations are presented in Tables 2 and 3 whereas scatterplots showing the overall relationships are presented in Figures 5 and 6.

3 | RESULTS

3.1 | NAc seed–ROI rsFC

Both the tinnitus and control subjects exhibited a high degree of connectivity between our NAc seed regions and the ROIs of the AAL2 atlas, as seen in Figure 2. Subtraction analysis of the two groups (Figure 3) reveals that, although both groups feature a high degree of NAc-related connectivity, there are large differences in terms of individual connection strength. The greatest increases in strength in tinnitus subjects relative to controls (Figure 3, warm colors) are in connections with the ventral and orbital regions of frontal cortex as well as inferior temporal cortex. The greatest decreases in strength in tinnitus subjects relative to controls (Figure 3, cool colors) are in lateral frontal cortex, the medial temporal lobe (incl. the amygdala), and the cerebellum.

3.2 | NAc seed–voxel rsFC

Voxelwise analyses using left/right NAc as seed regions (Figure 4) revealed rsFC throughout the entire brain in the tinnitus subjects, with the greatest effect sizes observed in the ventral and orbital regions of frontal cortex, incl. sgACC. In the control subjects, however, connectivity was mainly localized to the voxels in and immediately around the seed region. Subtraction analysis of the two groups reveals that the significant differences in NAc-related voxelwise connectivity are mainly localized in the aforementioned regions of ventral/orbital frontal cortex. We additionally observed significant group-level differences in connectivity between left NAc and (a) the inferior temporal gyrus, extending posteriorly into the occipital lobe, (b) the left superior frontal gyrus, and (c) the cerebellum. Differences in right NAc-related connectivity beyond ventral/orbital frontal cortex were limited to the left superior frontal gyrus, in roughly the same location as observed in left NAc.

3.3 | NAc rsFC correlation analysis

RsFC between NAc and tinnitus-related brain regions (see Section 2.5.4) correlated with some of the behavioral measures of the tinnitus group. Frontoatrial connections (i.e., NAc–vmPFC) correlated negatively with age, mean hearing loss, and tinnitus percept loudness.

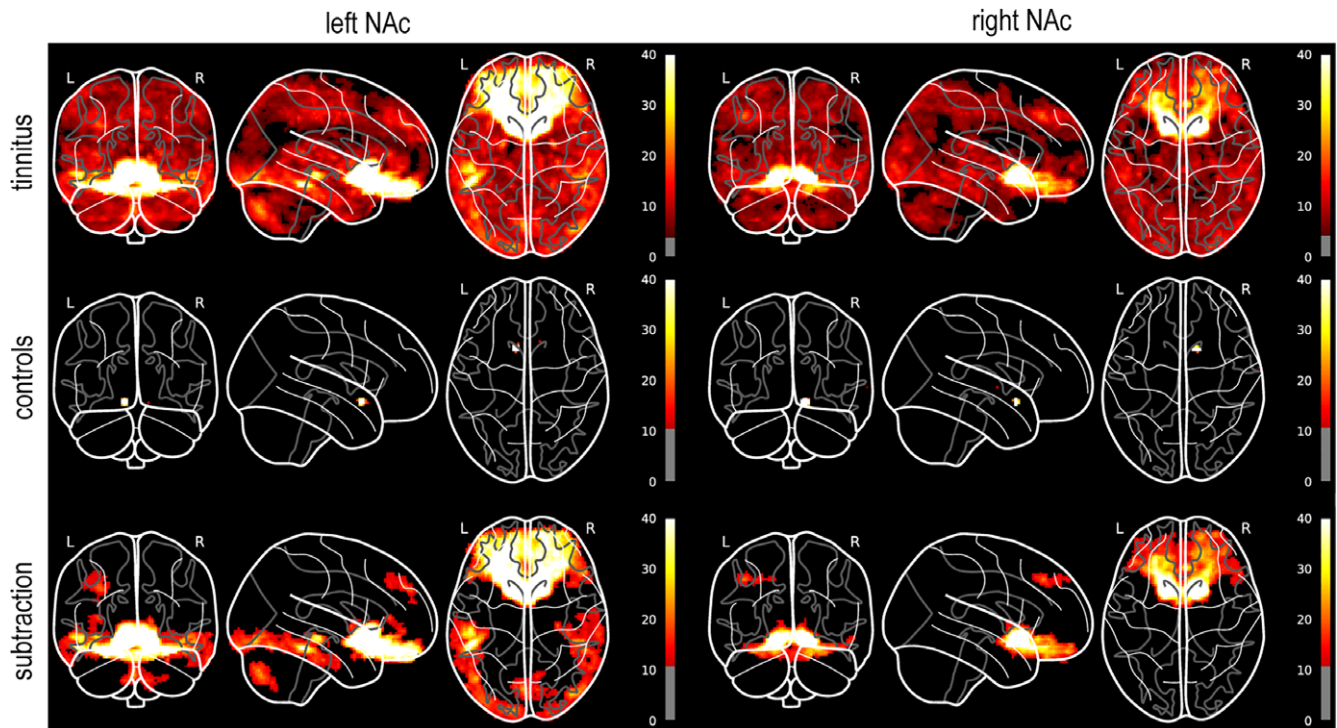


FIGURE 4 Glass-brain visualizations of voxelwise rsFC with left/right NAc seed regions. All analyses include age and whole-brain rsFC as covariates. The within-group results for the tinnitus and control subjects (top, middle) are presented at height thresholds of $p < 0.05$ and cluster thresholds of $p < 0.05$, both including the FDR correction for multiple comparisons. The subtraction analysis (bottom) is presented at a height threshold of $p = 0.0001$ (uncorrected) and a cluster threshold of 200 voxels. These height thresholds are reflected by the grayed-out regions of each colorbar. The colorbar range over all subfigures has also been restricted to a maximum height of 40 (F -statistic) both for the purposes of direct visual comparison and also to better display the overall variance in the data; the true maxima of the subfigures are much higher, owing to the high correlations of the seed regions with the voxels in and around them [Color figure can be viewed at wileyonlinelibrary.com]

TABLE 2 Significant correlations between NAc-related rsFC and tinnitus patient characteristics

Connection	Variable	r	p
NAc _R -vmPFC _L	Age	-0.253	0.016
NAc _R -vmPFC _R	Age	-0.242	0.022
NAc _R -vmPFC _R	Hearing loss	-0.288	0.006
NAc _R -vmPFC _R	Loudness	-0.255	0.015
NAc _L -PHC _L	Loudness	0.360	<0.001
NAc _L -PHC _L	Duration	0.254	0.016
NAc _R -pgACC _L	Duration	-0.208	0.049

All of these negative correlations specifically involved NAc_R-vmPFC_R, though NAc_R-vmPFC_L did also correlate with age. NAc_L-PHC_L rsFC correlated positively with both tinnitus percept loudness and the duration of tinnitus symptoms. Finally, NAc_R-pgACC_L correlated negatively with duration. See Table 2 for these results and Figure 5 for corresponding scatterplots.

After running a partial correlation analysis controlling for the effects of age and mean hearing loss, the correlations between NAc_L-PHC_L and loudness/duration remained significant. A significant correlation between NAc_R-vmPFC_L and duration also appeared. The partial correlation between NAc_L-PHC_L and loudness also survived FDR correction for multiple comparisons. See Table 3 for these results and Figure 6 for corresponding scatterplots. The full results for all tested

TABLE 3 Partial correlations between NAc-related rsFC and tinnitus patient characteristics, controlling for age and mean hearing loss

Connection	Variable	r_{partial}	p
NAc _L -PHC _L	Loudness	0.372	<0.001*
NAc _L -PHC _L	Duration	0.254	0.014
NAc _R -vmPFC _L	Duration	0.218	0.041

Asterisks indicate p values that survive FDR correction for multiple comparisons.

correlations and partial correlations are presented in Supporting Information.

4 | DISCUSSION

Our present results indicated that NAc features significant rsFC in subjects with chronic tinnitus. This NAc rsFC was reduced or absent in healthy subjects and this difference was not due to age, the most likely confound. As expected, the greatest level of NAc rsFC in the tinnitus subjects involved vmPFC, OFC, and sgACC. However, connectivity with NAc also extended throughout cerebral and cerebellar cortex. Furthermore, NAc-related rsFC correlated with both tinnitus percept loudness and the duration of tinnitus symptoms after controlling for the effects of age and mean hearing loss. We will discuss our

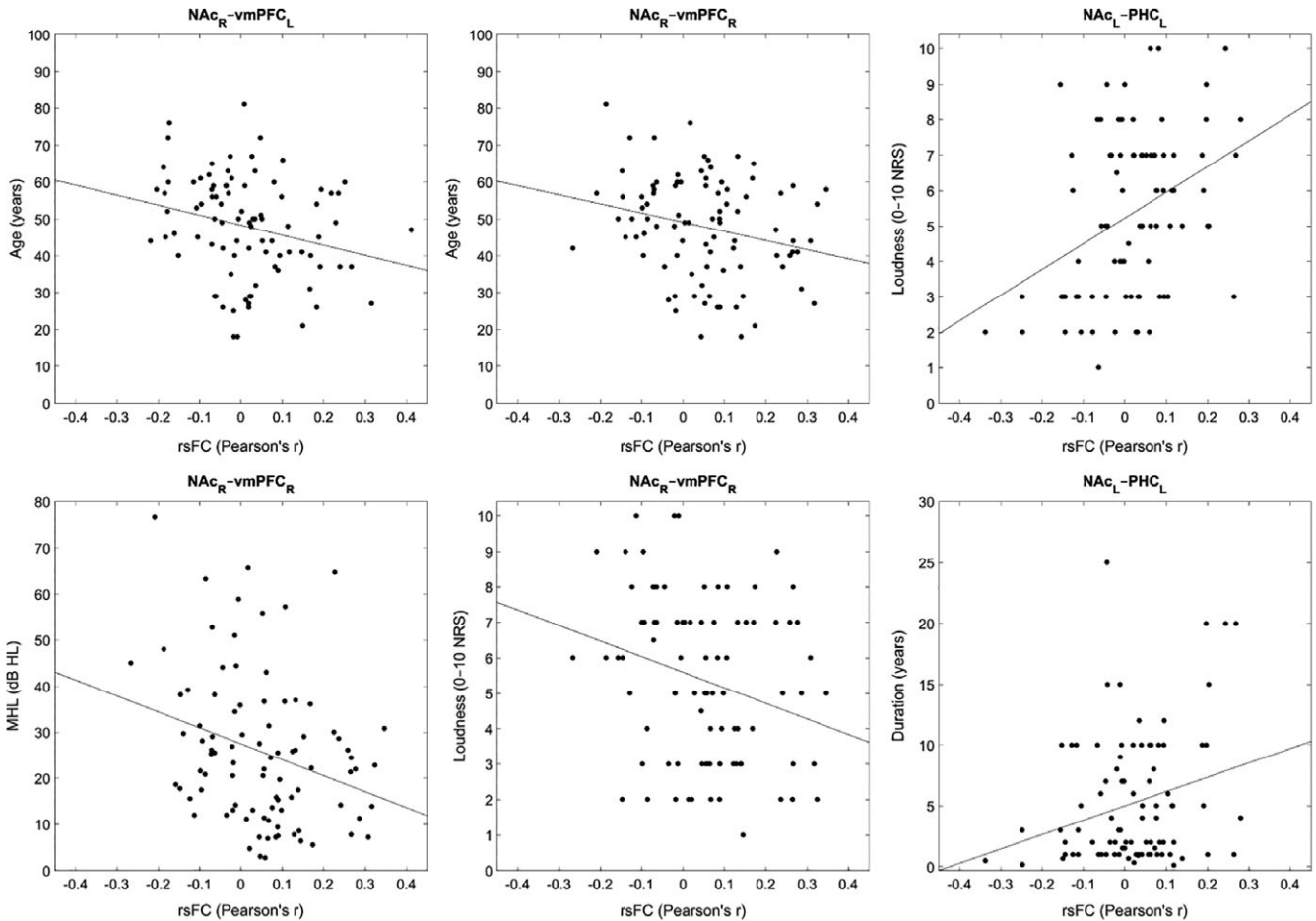


FIGURE 5 Scatterplots displaying the NAc-related rsFC and tinnitus patient characteristics with significant correlations

findings here in the context of the current literature to build a hypothesis on the role of NAc in tinnitus.

Our atlas-based rsFC analyses indicated not only that both tinnitus and control subjects featured widespread connectivity with NAc (Figure 2) but also that there were distinct patterns of connectivity in each group (Figure 3). Voxelwise analyses of NAc-related rsFC told a

somewhat different story, however (Figure 4). We still observed rsFC between NAc and the whole brain in tinnitus subjects but the rsFC in control subjects disappeared almost entirely. Subtraction analysis of the voxelwise results was nevertheless partially consistent with the analogous ROI-based analysis, with differences in rsFC located in ventral and orbital frontal cortex, inferior temporal and occipital cortex,

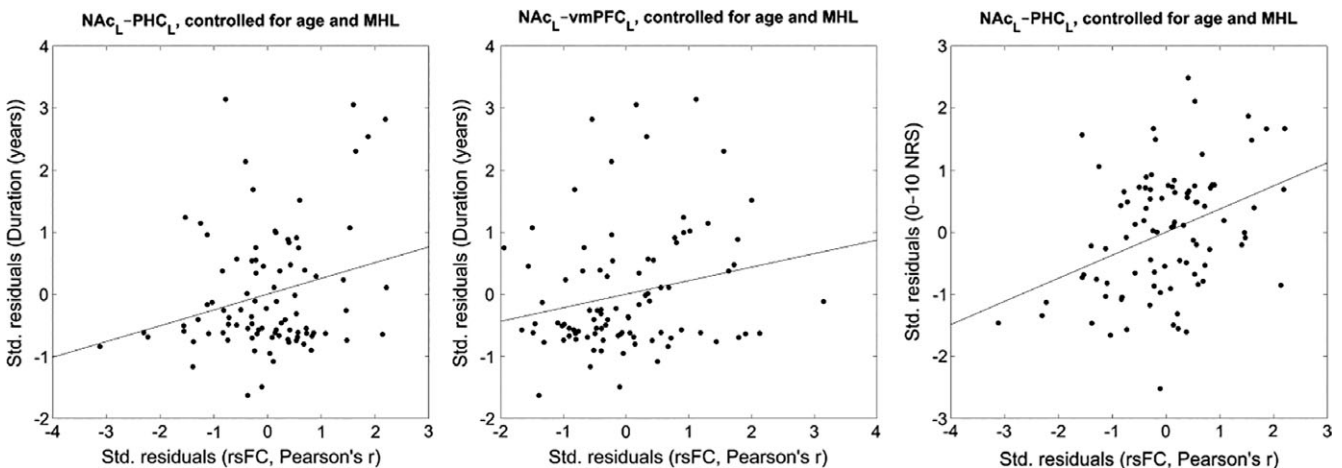


FIGURE 6 Scatterplots displaying the NAc-related rsFC and tinnitus patient characteristics with significant partial correlations, controlling for the effects of age and mean hearing loss. Axes display the standardized residuals in each variable after regressing them onto tinnitus patient age and mean hearing loss

and the cerebellum. Again, however, note that these differences were all greater for tinnitus subjects than controls; there were no significant differences where control subjects had greater voxelwise rsFC than tinnitus subjects. The implication is therefore that NAc does feature strong rsFC throughout the brains of tinnitus subjects but that this connectivity can be obscured by the choice of atlas. Indeed, while the control subjects saw the biggest change, both groups saw reductions in rsFC in the voxelwise analyses relative to the ROI-based analyses. Future studies conducting ROI-based analyses should therefore consider other atlases—ideally, at least two simultaneously—and should also include voxelwise analyses in tandem to mitigate the potential biases introduced by defining ROIs.

The general observation that NAc features connectivity with orbital and ventromedial frontal areas is broadly consistent with the literature identifying those areas as primary targets of NAc afferents (Cauda et al., 2011). The specific observation that this frontostriatal connectivity is increased in tinnitus subjects relative to healthy subjects has only been discussed in tinnitus by a few researchers (Leaver et al., 2011; Leaver et al., 2016; Rauschecker et al., 2015) but it is consistent with literature from analogous disorders such as chronic pain (Apkarian et al., 2011; Baliki et al., 2012). NAc is also implicated in the pathologies of several other disorders, namely so-called reward deficiency syndromes, which include addiction, attention deficit hyperactivity disorder, and schizophrenia, among others; see e.g., (Blum et al., 2000). Finally, NAc is part of the salience network anchored in dorsal anterior cingulate cortex and anterior insular cortex (Seeley et al., 2007). This network has been identified as a common substrate of most neurological and psychiatric disorders (Downar, Blumberger, & Daskalakis, 2016; Goodkind et al., 2015; Peters, Dunlop, & Downar, 2016). The observed connectivity involving NAc in tinnitus may therefore be interpreted in the context of salience, although this merits direct testing in future studies.

Our various rsFC analyses indicated that tinnitus subjects have increased NAc-related connectivity relative to that of healthy subjects. Furthermore, these results were controlled for the effects of age and whole-brain rsFC, which we included as a covariate in all analyses. To directly test whether these increases were actually due to tinnitus, as opposed to some other, confounding factor, we performed correlation analyses between NAc-related rsFC and several behavioral measures unique to tinnitus (Figures 5 and 6; Tables 2 and 3). In particular, we were interested in testing whether the NAc-related connectivity observed in tinnitus patients fit with the predictions of existing pathological models, namely frontostriatal gating (Leaver et al., 2011; Leaver et al., 2016; Rauschecker et al., 2015). Our results however indicated no significant correlation between NAc-vmPFC or NAc-sgACC and tinnitus-related distress, contrary to what we expected given existing literature (Apkarian et al., 2011; Baliki et al., 2006; Rauschecker et al., 2015). There was a negative correlation between NAc-vmPFC and tinnitus percept loudness, but this result did not survive correction for multiple comparisons and it disappeared when controlling for the effects of age and mean hearing loss. While we do not observe direct evidence supporting the predictions of the frontostriatal gating theory, it is possible that frontostriatal circuits are indirectly involved in sensory gating. For example, the strongest correlation we observed was between NAc-PHC and tinnitus percept loudness, which did

survive correction for multiple comparisons after controlling for the effects of age and mean hearing loss. A modified frontostriatal gating theory—one where PHC is a potential generator of tinnitus signals and part of the extended network—could therefore still be valid in the context of our present results. Recent research has indeed shown that PHC can be a tinnitus generator, especially in cases where the patient has severe hearing loss; see e.g., (De Ridder, Vanneste, & Freeman, 2014a; Sedley et al., 2015; Vanneste, van de Heyning, & de Ridder, 2011; Vanneste & De Ridder, 2016). The relevant question for frontostriatal gating is whether NAc interacts with PHC independently from its involvement with vmPFC/sACC, which is a valuable topic for future studies.

Given that we did see correlations between NAc-related connectivity and tinnitus measures but that our findings do not necessarily fit with the frontostriatal gating theory, we are left to look elsewhere in the literature for an explanation of our results. From the pain literature, for example, we know that increased NAc-mPFC functional connectivity predicts pain persistence, implying a causal relationship between frontostriatal circuits and the transition from acute to chronic pain (Baliki et al., 2012). We observed a similar correlation in our own results, namely between frontostriatal connectivity (NAc-vmPFC) and the duration of tinnitus symptoms after controlling for the effects of age and mean hearing loss. Given the well-established similarities between tinnitus and chronic pain (Møller, 2011; Rauschecker et al., 2015; De Ridder et al., 2011), we hypothesize that frontostriatal connectivity predicts the transition from acute to chronic tinnitus. Direct testing of this hypothesis is a matter for future research, given that the analogous finding from the pain literature was based on a longitudinal study (Baliki et al., 2012) while our present study only observed tinnitus patients who were already in the chronic stage.

4.1 | Limitations

There are a few limitations of the present study worth mentioning both as caveats and as prompts for future research. The first and most obvious is the difference in scanning protocols between our tinnitus and control groups. While we did take steps to minimize any impact this may have had on our present results (see e.g., Section 2.5.1), a purpose-built data set that used the same protocol to scan both groups would be useful for verification. The other limitation is that we did not correct for potential distortions of our MR images during the normalization step of our preprocessing pipeline.

5 | CONCLUSIONS

Our findings showed significant involvement of NAc in the brains of tinnitus patients. We observed connectivity with NAc throughout diverse regions of the brain, while healthy subjects exhibited significantly less NAc-related connectivity. Furthermore, NAc-related connectivity correlated significantly with tinnitus percept loudness and the duration of tinnitus symptoms even after controlling for the effects of age and mean hearing loss, which were the two most likely confounds. However, while our present study shows that NAc plays some role in the pathology of tinnitus, future research will be

necessary to determine the specifics of this role. We hypothesize that NAc is involved in the transition from acute to chronic phantom perception, based on the analogous finding from the pain literature (Baliki et al., 2012). This is consistent with the well-established general role of NAc in both normal and pathological learning; see e.g., (Chang et al., 2014; Donoso et al., 2014; Koechlin, 2016; Takahashi et al., 2008; Takahashi et al., 2017). The implication of this, if confirmed, is that chronic phantom perception in multiple sensory domains—auditory, nociceptive, and quite possibly others—is mediated in part by maladaptive learning processes in frontostriatal circuits. This may further imply a shared neural substrate with so-called reward deficiency syndromes including addiction, attention deficit hyperactivity disorder, schizophrenia, and others; see e.g., (Blum et al., 2000). Ultimately, our present results are consistent with a larger trend showing common neural features across several different aspects of normal and disordered brain function (Downar et al., 2016; Goodkind et al., 2015; Peters et al., 2016).

ACKNOWLEDGMENTS

Research by Jeffrey Hullfish is supported by the Eugene McDermott Graduate Fellowship (201501). Data were provided in part by the Human Connectome Project, WU-Minn Consortium (Principal Investigators: David Van Essen and Kamil Ugurbil; 1U54MH091657) funded by the 16 NIH Institutes and Centers that support the NIH Blueprint for Neuroscience Research; and by the McDonnell Center for Systems Neuroscience at Washington University.

CONFLICT OF INTERESTS

The authors declare no competing financial interests.

ORCID

Jeffrey Hullfish  <https://orcid.org/0000-0002-2536-9491>

REFERENCES

- Apkarian, A. V., Hashmi, J. A., & Baliki, M. N. (2011). Pain and the brain: Specificity and plasticity of the brain in clinical chronic pain. *Pain*, *152*, S49–S64.
- Ashburner, J., & Friston, K. J. (1999). Nonlinear spatial normalization using basis functions. *Human Brain Mapping*, *7*, 254–266.
- Baliki, M. N., Chialvo, D. R., Geha, P. Y., Levy, R. M., Harden, R. N., Parrish, T. B., & Apkarian, A. V. (2006). Chronic pain and the emotional brain: Specific brain activity associated with spontaneous fluctuations of intensity of chronic back pain. *The Journal of Neuroscience*, *26*, 12165–12173.
- Baliki, M. N., Petre, B., Torbey, S., Herrmann, K. M., Huang, L., Schnitzer, T. J., ... Apkarian, A. V. (2012). Corticostriatal functional connectivity predicts transition to chronic back pain. *Nature Neuroscience*, *15*, 1117–1119.
- Becerra, L., & Borsook, D. (2008). Signal valence in the nucleus accumbens to pain onset and offset. *European Journal of Pain*, *12*, 866–869.
- Behzadi, Y., Restom, K., Liu, J., & Liu, T. T. (2007). A component based noise correction method (CompCor) for BOLD and perfusion based fMRI. *NeuroImage*, *37*, 90–101.
- Blum, K., Braverman, E. R., Holder, J. M., Lubar, J. F., Monastra, V. I., Miller, D., ... Comings, D. E. (2000). The reward deficiency syndrome: A biogenetic model for the diagnosis and treatment of impulsive, addictive and compulsive behaviors. *Journal of Psychoactive Drugs*, *32*, 1–112.
- British Society of Audiology. (2017). *Recommended procedure: Pure-tone air-conduction and bone-conduction threshold audiometry with and without masking*. British Society of Audiology. <http://www.thebsa.org.uk/wp-content/uploads/2017/02/Recommended-Procedure-Pure-Tone-Audiometry-Jan-2017-V2-1.pdf>.
- Cauda, F., Cavanna, A. E., D'agata, F., Sacco, K., Duca, S., & Geminiani, G. C. (2011). Functional connectivity and coactivation of the nucleus accumbens: A combined functional connectivity and structure-based meta-analysis. *Journal of Cognitive Neuroscience*, *23*, 2864–2877.
- Chang, P. C., Pollema-Mays, S. L., Centeno, M. V., Proccissi, D., Contini, M., Baria, A. T., ... Apkarian, A. V. (2014). Role of nucleus accumbens in neuropathic pain: Linked multi-scale evidence in the rat transitioning to neuropathic pain. *Pain*, *155*, 1128–1139.
- Donoso, M., Collins, A. G. E., & Koechlin, E. (2014). Foundations of human reasoning in the prefrontal cortex. *Science*, *344*, 1481–1486.
- Downar, J., Blumberger, D. M., & Daskalakis, Z. J. (2016). The neural crossroads of psychiatric illness: An emerging target for brain stimulation. *Trends in Cognitive Sciences*, *20*, 107–120.
- Elgoyhen, A. B., Langguth, B., De Ridder, D., & Vanneste, S. (2015). Tinnitus: Perspectives from human neuroimaging. *Nature Reviews. Neuroscience*, *16*, 632–642.
- Van Essen, D. C., Ugurbil, K., Auerbach, E., Barch, D., Behrens, T. E. J., Bucholz, R., ... Yacoub, E. (2012). The human connectome project: A data acquisition perspective. *NeuroImage*, *62*, 2222–2231.
- Friston, K., Ashburner, J., Frith, C. D., Poline, J., Heather, J. D., & Frackowiak, R. S. J. (1995). Spatial registration and normalization of images. *Human Brain Mapping*, *3*, 165–189.
- Glasser, M. F., Sotiropoulos, S. N., Wilson, J. A., Coalson, T. S., Fischl, B., Andersson, J. L., ... Jenkinson, M. (2013). The minimal preprocessing pipelines for the human connectome project. *NeuroImage*, *80*, 105–124.
- Goodkind, M., Eickhoff, S. B., Oathes, D. J., Jiang, Y., Chang, A., Jones-Hagata, L. B., ... Etkin, A. (2015). Identification of a common neurobiological substrate for mental illness. *JAMA Psychiatry*, *72*, 305–315.
- Hallam, R. S., Jakes, S. C., & Hinchcliffe, R. (1988). Cognitive variables in tinnitus annoyance. *The British Journal of Clinical Psychology*, *27*(Pt 3), 213–222.
- Hochberg, Y., & Benjamini, Y. (1995). Controlling the false discovery rate: A practical and powerful approach to multiple testing. *Journal of the Royal Statistical Society*, *57*, 289–300.
- IBM Corp. (2013). *IBM SPSS statistics for windows*. Armonk, NY: IBM Corp.
- Kahn, I., & Shohamy, D. (2013). Intrinsic connectivity between the hippocampus, nucleus accumbens, and ventral tegmental area in humans. *Hippocampus*, *23*, 187–192.
- Keiflin, R., & Janak, P. H. (2015). Dopamine prediction errors in reward learning and addiction: From theory to neural circuitry. *Neuron*, *88*, 247–263.
- Koechlin, E. (2016). Prefrontal executive function and adaptive behavior in complex environments. *Current Opinion in Neurobiology*, *37*, 1–6.
- Lamm, S., Lim, B. K., Ran, C., Huang, K. W., Betley, M. J., Tye, K. M., ... Malenka, R. C. (2012). Input-specific control of reward and aversion in the ventral tegmental area. *Nature*, *491*, 212–217.
- Leaver, A. M., Renier, L., Chevillet, M. A., Morgan, S., Kim, H. J., & Rauschecker, J. P. (2011). Dysregulation of limbic and auditory networks in tinnitus. *Neuron*, *69*, 33–43.
- Leaver, A. M., Turesky, T. K., Seydell-Greenwald, A., Morgan, S., Kim, H. J., & Rauschecker, J. P. (2016). Intrinsic network activity in tinnitus investigated using functional MRI. *Human Brain Mapping*, *37*, 2717–2735.
- Liu, X., Hairston, J., Schrier, M., & Fan, J. (2011). Common and distinct networks underlying reward valence and processing stages: A meta-analysis of functional neuroimaging studies. *Neuroscience and Biobehavioral Reviews*, *35*, 1219–1236.
- Meeus, O., Blaivie, C., & Van De Heyning, P. (2007). Validation of the Dutch and the French version of the tinnitus questionnaire. *B-Ent*, *3*, 11–17.
- Mohan, A., & Vanneste, S. (2017). Adaptive and maladaptive neural compensatory consequences of sensory deprivation—From a phantom percept perspective. *Progress in Neurobiology*, *153*, 1–17.
- Møller, A. R. (2011). Similarities between tinnitus and pain. In *Textbook of tinnitus* (pp. 113–120). New York, NY: Springer New York.
- Navratilova, E., Xie, J. Y., Okun, A., Qu, C., Eyde, N., Ci, S., ... Porreca, F. (2012). Pain relief produces negative reinforcement through activation

- of mesolimbic reward-valuation circuitry. *Proceedings of the National Academy of Sciences of the United States of America*, 109, 20709–20713.
- Peters, S. K., Dunlop, K., & Downar, J. (2016). Cortico-striatal-thalamic loop circuits of the salience network: A central pathway in psychiatric disease and treatment. *Frontiers in Systems Neuroscience*, 10, 1–23.
- Rauschecker, J. P., May, E. S., Maudoux, A., & Ploner, M. (2015). Frontostriatal gating of tinnitus and chronic pain. *Trends in Cognitive Sciences*, 19, 567–578.
- De Ridder, D., Elgoyhen, A. B., Romo, R., & Langguth, B. (2011). Phantom percepts: Tinnitus and pain as persisting aversive memory networks. *Proceedings of the National Academy of Sciences of the United States of America*, 108, 8075–8080.
- De Ridder, D., Vanneste, S., & Freeman, W. (2014a). The Bayesian brain: Phantom percepts resolve sensory uncertainty. *Neuroscience and Biobehavioral Reviews*, 44, 4–15.
- De Ridder, D., Vanneste, S., Gillett, G., Manning, P., Glue, P., & Langguth, B. (2016). Psychosurgery reduces uncertainty and increases free will? A review. *NeuroModulation*, 19, 239–248.
- De Ridder, D., Vanneste, S., Weisz, N., Londero, A., Schlee, W., Elgoyhen, A. B., & Langguth, B. (2014b). An integrative model of auditory phantom perception: Tinnitus as a unified percept of interacting separable subnetworks. *Neuroscience and Biobehavioral Reviews*, 44, 16–32.
- Rolland, B., Amad, A., Poulet, E., Bordet, R., Vignaud, A., Bation, R., ... Jardri, R. (2015). Resting-state functional connectivity of the nucleus accumbens in auditory and visual hallucinations in schizophrenia. *Schizophrenia Bulletin*, 41, 291–299.
- Rolls, E. T., Joliot, M., & Tzourio-Mazoyer, N. (2015). Implementation of a new parcellation of the orbitofrontal cortex in the automated anatomical labeling atlas. *NeuroImage*, 122, 1–5.
- Salimi-Khorshidi, G., Douaud, G., Beckmann, C. F., Glasser, M. F., Griffanti, L., & Smith, S. M. (2014). Automatic denoising of functional MRI data: Combining independent component analysis and hierarchical fusion of classifiers. *NeuroImage*, 90, 449–468.
- Schiffman, A. M., Waszak, F., & Yeung, N. (2015). The role of prediction and outcomes in adaptive cognitive control. *Journal of Physiology, Paris*, 109, 38–52.
- Sedley, W., Friston, K. J., Gander, P. E., Kumar, S., & Griffiths, T. D. (2016). An integrative tinnitus model based on sensory precision. *Trends in Neurosciences*, 39, 799–812.
- Sedley, W., Gander, P. E., Kumar, S., Oya, H., Kovach, C. K., Nourski, K. V., ... Griffiths, T. D. (2015). Intracranial mapping of a cortical tinnitus system using residual inhibition. *Current Biology*, 25, 1208–1214.
- Seeley, W. W., Menon, V., Schatzberg, A. F., Keller, J., Glover, G. H., Kenna, H., ... Greicius, M. D. (2007). Dissociable intrinsic connectivity networks for salience processing and executive control. *The Journal of Neuroscience*, 27, 2349–2356.
- Smith, S. M., Beckmann, C. F., Andersson, J., Auerbach, E. J., Bijsterbosch, J., Douaud, G., ... Glasser, M. F. (2013). Resting-state fMRI in the human connectome project. *NeuroImage*, 80, 144–168.
- Takahashi, Y. K., Batchelor, H. M., Liu, B., Khanna, A., Morales, M., & Schoenbaum, G. (2017). Dopamine neurons respond to errors in the prediction of sensory features of expected rewards. *Neuron*, 95, 1395–1405.e3.
- Takao, Y., Schoenbaum, G., & Niv, Y. (2008). Silencing the critics: Understanding the effects of cocaine sensitization on dorsolateral and ventral striatum in the context of an actor/critic model. *Frontiers in Neuroscience*, 2, 86–89.
- Tonnendorf, J. (1987). The analogy between tinnitus and pain: A suggestion for a physiological basis of chronic tinnitus. *Hearing Research*, 28, 271–275.
- Tzourio-Mazoyer, N., Landeau, B., Papathanassiou, D., Crivello, F., Etard, O., Delcroix, N., ... Joliot, M. (2002). Automated anatomical labeling of activations in SPM using a macroscopic anatomical parcellation of the MNI MRI single-subject brain. *NeuroImage*, 15, 273–289.
- Uğurbil, K., Xu, J., Auerbach, E. J., Moeller, S., Vu, A. T., Duarte-Carvajalino, J. M., ... Yacoub, E. (2013). Pushing spatial and temporal resolution for functional and diffusion MRI in the human connectome project. *NeuroImage*, 80, 80–104.
- Vanneste, S., van de Heyning, P., & de Ridder, D. (2011). The neural network of phantom sound changes over time: A comparison between recent-onset and chronic tinnitus patients. *The European Journal of Neuroscience*, 34, 718–731.
- Vanneste, S., & De Ridder, D. (2016). Deafferentation-based pathophysiological differences in phantom sound: Tinnitus with and without hearing loss. *NeuroImage*, 129, 80–94.
- Vanneste, S., Song, J. J., & De Ridder, D. (2013). Tinnitus and musical hallucinosis: The same but more. *NeuroImage*, 82, 373–383.
- Whitfield-Gabrieli, S., & Nieto-Castanon, A. (2012). Conn: A functional connectivity toolbox for correlated and anticorrelated brain networks. *Brain Connectivity*, 2, 125–141.
- World Medical Association. (2000). Declaration of Helsinki, ethical principles for medical research involving human subjects. *52nd WMA General Assembly*. Edinburgh, Scotland.
- Zhang, S., & Li, C.-S. R. (2014). Functional clustering of the human inferior parietal lobule by whole-brain connectivity mapping of resting-state functional magnetic resonance imaging signals. *Brain Connectivity*, 4, 53–69.

SUPPORTING INFORMATION

Additional supporting information may be found online in the Supporting Information section at the end of the article.

How to cite this article: Hullfish J, Abenes I, Yoo HB, De Ridder D, Vanneste S. Frontostriatal network dysfunction as a domain-general mechanism underlying phantom perception. *Hum Brain Mapp*. 2019;1–11. <https://doi.org/10.1002/hbm.24521>